Finite element analysis of absorption characteristics of permeable membrane absorbers array

Uenishi, Koji
Okuzono, Takeshi
Sakagami, Kimihiro

(Citation)
Acoustical Science and Technology,38(6):322-325

(Issue Date)
2017-11-01

(Resource Type)
journal article

(Version)
Version of Record

(URL)
https://hdl.handle.net/20.500.14094/90005903

ACOUSTICAL LETTER

Finite element analysis of absorption characteristics of permeable membrane absorbers array

Koji Uenishi, Takeshi Okuzono* and Kimihiro Sakagami

Environmental Acoustic Laboratory, Department of Architecture, Graduate School of Engineering, Kobe University, 1–1 Rokkodai, Nada-ku, Kobe, 657–8501 Japan

(*Received 11 May 2017, Accepted for publication 30 May 2017*)

Keywords: Permeable membrane, Normal incidence sound absorption coefficient, Acoustic intensity, Excess sound absorption, Finite element method

PACS number: 43.55.Ev, 43.55.Dt, 43.55.Ka [doi:10.1250/ast.38.322]

1. Introduction

Permeable membranes (PM), which are usually made of a core textile coated with resin, have been recognized as attractive sound absorbing materials for controlling acoustical condition in rooms because of their light transmissibility, designability and lightweight properties. From a view point of acoustics, they have flow resistance suitable for sound absorption purpose, and they can absorb sound energy by their acoustic resistance. Various PM absorbers have been developed with the attractive features [1,2]. The simplest absorber is a single-leaf absorber (SG) as shown in Fig. 1(a), in which a PM is placed in front of a rigid-backed air cavity. The air cavity can be partitioned using honeycomb core (HC) as shown in Fig. 1(b). The locally reacting air cavity has a favorable effect for field incidence absorption coefficients. By the effect of air cavity, HC shows higher absorption at lower frequencies [3]. However, as a disadvantage, notch with zero absorption occurs at particular frequency for any incident angles because the locally reacting air cavity has infinite impedance at the frequencies, $f_n = (c_0/2D) \times n$ $(n = 1, 2, \ldots)$ [3], where c_0 and D represent the speed of sound and air cavity depth, respectively.

A solution for the above deficiency of HC is PM absorbers array (AR) as shown in Fig. 1(c), which uses multiple locally reacting air cavities with different depths so that each cavity has different notch frequencies. In this paper, we investigate the absorption characteristics of AR using two-dimensional frequency domain finite element (FE) analyses. The present study focuses on how the absorption of each PM absorber component with different cavity depths contributes the overall absorption of AR, in the relation with material property of PM. For that purpose, we analyze (i) sound energy dissipated by each PM absorber that constructs AR, (ii) particle velocity distributions on the surface of each PM absorber, and (iii) acoustic intensity flow to the absorber.

2. Outline of FE analysis

2.1. Setup of FE analyses

The normal incidence absorption coefficients α_N of SG, HC and AR were calculated using an impedance tube model in the frequency range from 1 Hz to 2,830 Hz with 1 Hz interval. Figure 2 shows the impedance tube model for the calculation of AR. In the calculation of α_N of SG, HC and AR, the speed of sound c_0 and air density ρ_0 were respectively assumed to be 343.7 m/s and 1.205 kg/m^3. Air domains were discretized using four node quadrilateral FEs with modified integration rules [4] for reducing dispersion errors. PM was modeled using limp membrane FEs [5]. FE meshes were created using FEs with the length of 0.001 m. For HC and AR partitions were assumed to be rigid. The constant volume velocity of 1.0 m/s was given at the tube inlet. The tube inlet also has the characteristic impedance of air $\rho_0 c_0$.

2.2. Specification of PM absorbers

For SG and HC, their cavity depths D were set to 0.1 m. The first notch frequency is 1,718.5 Hz. For AR, three cavities with different depths were used and their cavity depths were respectively set to $D_1 = 0.05$ m, $D_2 = 0.1$ m, and $D_3 = 0.035$ m so that each component has different notch frequency. Note that hereafter each PM component with the cavity depth of D_1, D_2 and D_3 is defined respectively as ARsg50, ARsg100 and ARsg35. The widths W of HC and AR were set to 0.018 m so that sound waves propagate perpendicular to the absorber surfaces at the analyzed frequency range. For HC and AR, the partition thickness was set to 0.001 m. We used nine PMs with different surface density and flow resistance. The PMs have surface density M of 0.0625, 0.5, and 1.0 kg/m^2, each of which has flow resistance R_f of $0.125\rho_0 c_0$, $\rho_0 c_0$, and $2\rho_0 c_0$ Pa·s/m, respectively.

2.3. Calculation procedure of absorption coefficient

The normal incidence absorption coefficient is calculated as (See Ref. [6])

$$\alpha_N = \frac{W_{abs}}{W_{in}} = \frac{\int_0^h \mathrm{Re}[p_a^* \cdot u_a]dy}{[|p_{in}|^2/\rho_0 c_0] \cdot h} \tag{1}$$

where W_{in} and W_{abs} respectively represent the incident acoustic energy and absorbed energy. The symbols p_a, u_a and p_{in} represent, respectively, the sound pressure and particle velocity on absorber surface, and the sound pressure of incident plane wave. The values of h and y represent the height of impedance tube, and y direction in Fig. 2. The asterisk is the complex conjugate.

Sound energy dissipated by each PM absorber component is also calculated as (See Ref. [6])

*e-mail: okuzono@port.kobe-u.ac.jp

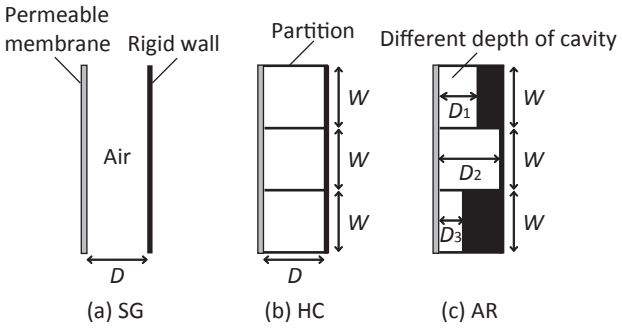

Fig. 1 Geometry of (a) SG, (b) HC and (c) AR. D, W are the depth and width of air cavity, respectively. In AR, D_i represent the depth of i-th cavity.

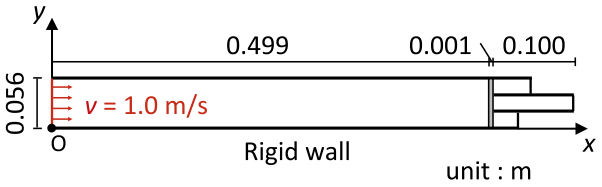

Fig. 2 Impedance tube model with AR.

$$\alpha_{\mathrm{N}}^{i} = \frac{W_{\mathrm{abs}}^{i}}{W_{\mathrm{in}}} \quad (i = 1, 2, 3) \tag{2}$$

where index i represent each PM absorber component of AR.

3. Results and discussion

3.1. Sound energy dissipated by each PM absorber component

Figure 3 shows comparison of absorption coefficients among SG·HC, ARsg50, ARsg100, ARsg35 and AR for the nine cases with different surface density and flow resistance values of PM. In all cases, AR shows higher absorption than SG·HC at the notch frequency thanks to the absorption of ARsg50 and ARsg35. Overall, AR shows higher absorption than SG·HC at almost all frequency ranges, but SG·HC have better performance at lower frequencies.

In the case with the lowest flow resistance $R_{\mathrm{f}} = 0.125\rho_0 c_0$, the surface density values do not have an influence on the absorption characteristics of AR. However, when the membrane's flow resistance is equal to $\rho_0 c_0$ or $2\rho_0 c_0$, the use of heavier membrane is effective to obtain higher absorption at lower frequencies.

Furthermore, we focus on the effect of material properties of PM on the absorption of ARsg's. When $M = 0.0625$ or $R_{\mathrm{f}} = 0.125\rho_0 c_0$, i.e., either M or R_{f} is relatively small, the absorption coefficient of each ARsg shows significantly higher value in narrow frequency band, and their values are higher than SG·HC. Also, the surfaces other than representative absorbing surface are reflective. The higher absorption in narrow frequency band can be considered as excess absorption [7] by the effect of large impedance discontinuity among ARsg surfaces. This is confirmed in particle velocity distributions on absorber surfaces and acoustic intensity flow, in subsequent sections. However, when the heavier membrane, i.e., $M = 0.5, 1.0$, is used, the excess absorption effect

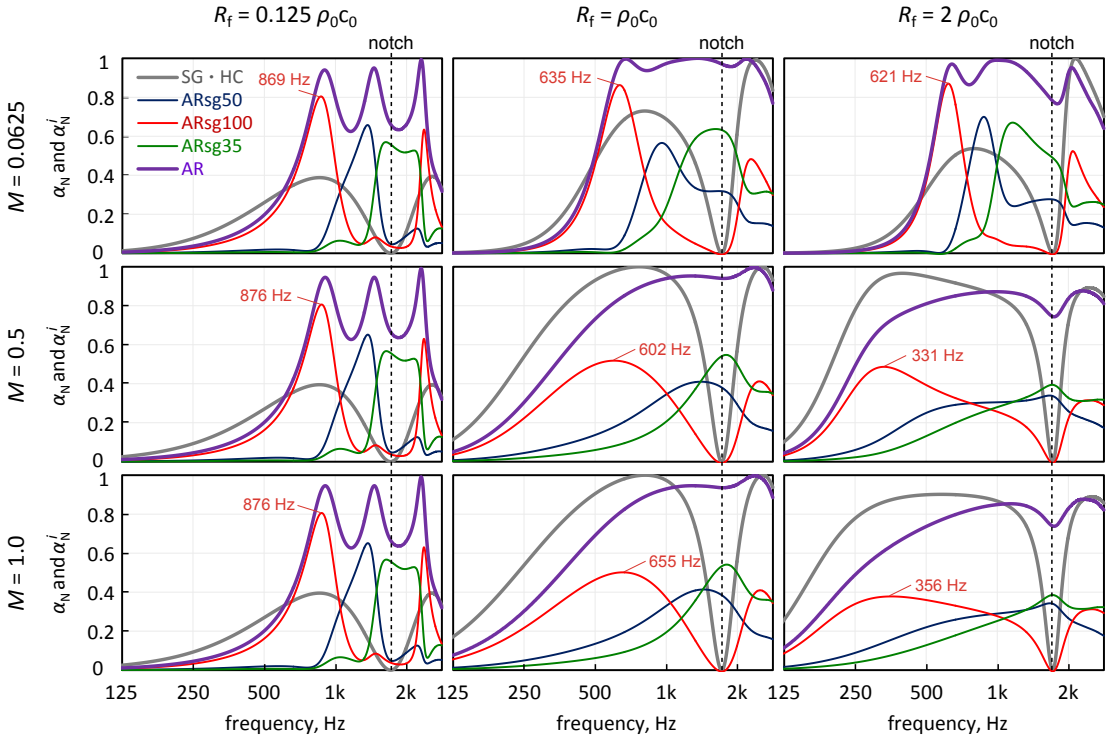

Fig. 3 α_{N} of AR and α_{N}^{i} of each PM absorber component in AR for the different values of M and R_{f}. α_{N} of SG and HC with 0.100 m air cavity is also shown for comparison. In Fig. 4, particle velocity distributions on the surface of AR are presented at peak frequencies of ARsg100 in above chart.

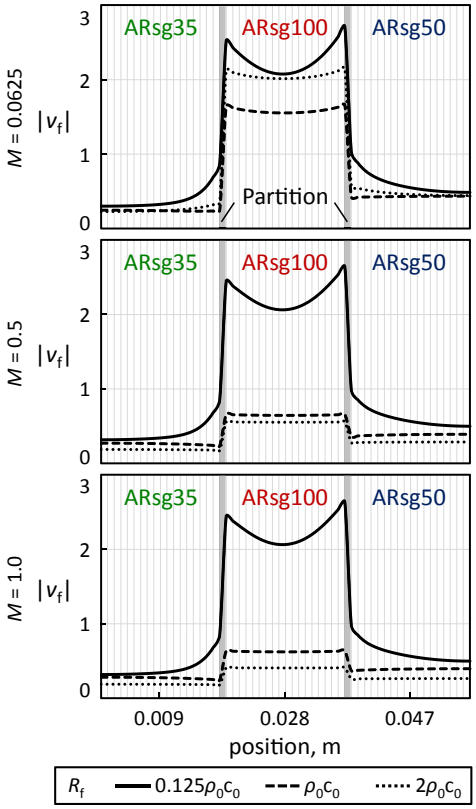

Fig. 4 Particle velocity distributions on surface of AR at which ARsg100 shows absorption peak. The peak frequencies are shown in Fig. 2.

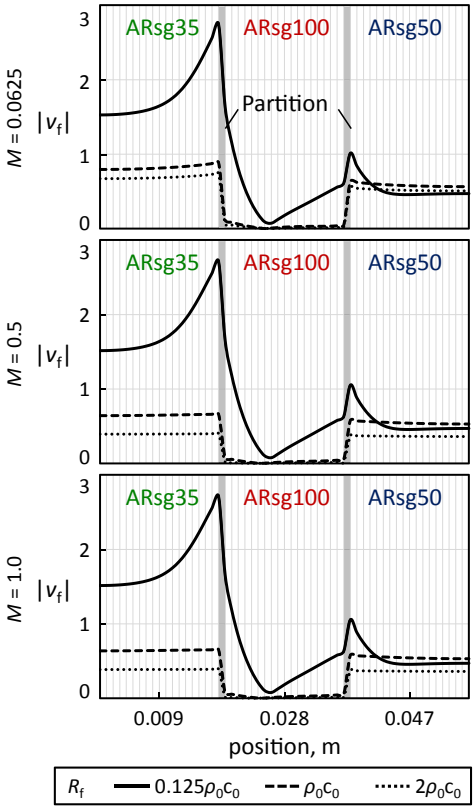

Fig. 5 Particle velocity distributions on surface of AR at which ARsg100 has notch at 1,718 Hz.

decreases with increasing flow resistance value. In that case, each ARsg shows a certain level of absorption in wider frequency ranges, and the value is lower than SG·HC.

3.2. Particle velocity distributions

Figures 4 and 5 respectively show the particle velocity distributions on surfaces of AR at frequencies, at which peak and notch occur in ARsg100. Here, the particle velocity is absolute values and a component normal to the absorber surface. In both cases, when $M = 0.0625$ or $R_f = 0.125\rho_0 c_0$, i.e., either M or R_f is small, the particle velocity on surface of each ARsg show higher value. In addition, the particle velocity difference among ARsg50, ARsg35 and ARsg100 is large. Furthermore, in the cases with the lowest flow resistance, the particle velocity shows the highest value near the partition. The spatial distributions of particle velocity on surfaces are non-uniform. As flow resistance increases, the particle velocity of each ARsg shows smaller value and the spatial distribution on each ARsg surface becomes uniform.

3.3. Acoustic intensity flow

Figures 6(a)–6(d) show acoustic intensity flow in the impedance tube at frequencies with peak and notch in ARsg100. The results are shown for the cases with $M = 0.0625$ and $R_f = 0.125\rho_0 c_0$ and $M = 1.0$ and $R_f = 2\rho_0 c_0$. The former is the case with excess absorption and the latter is not. The acoustic intensity was calculated at center of each finite element by using nodal sound pressure and particle velocity calculated from nodal pressure.

At the peak frequency, sound energy flow toward ARsg100 is stronger in the case with small material property of PM. At the notch frequency, sound energy flow directed to ARsg100 is weak, thus acts as reflective surface. However, the poor absorption is compensated by the absorption of ARsg50 and/or ARsg35. Clear sound energy flow toward ARsg50 and/or ARsg35 is observed.

4. Concluding and remarks

In this paper, the absorption characteristics of AR are investigated using two-dimensional frequency domain FE analyses. Within the range of investigated material properties, i.e., $0.0625 \leq M \leq 1.0$ and $0.125\rho_0 c_0 \leq R \leq 2\rho_0 c_0$, our findings are summarized below.

- AR overcomes the disadvantage of zero absorption at notch frequencies in SG and HC because zero absorptions of respective PM absorbers component are compensated each other by using multiple air cavities with different depths. However, SG and HC have better absorption performance at lower frequencies.
- When either surface density or flow resistance of PM is small, AR shows excess absorption. The particle velocity difference on surface of each ARsg is large. In that case, the absorption coefficient of each ARsg shows significantly higher value in narrow frequency band than SG and HC because of large impedance discontinuity among the surfaces of ARsg.
- When heavier membrane is used and the flow resistance

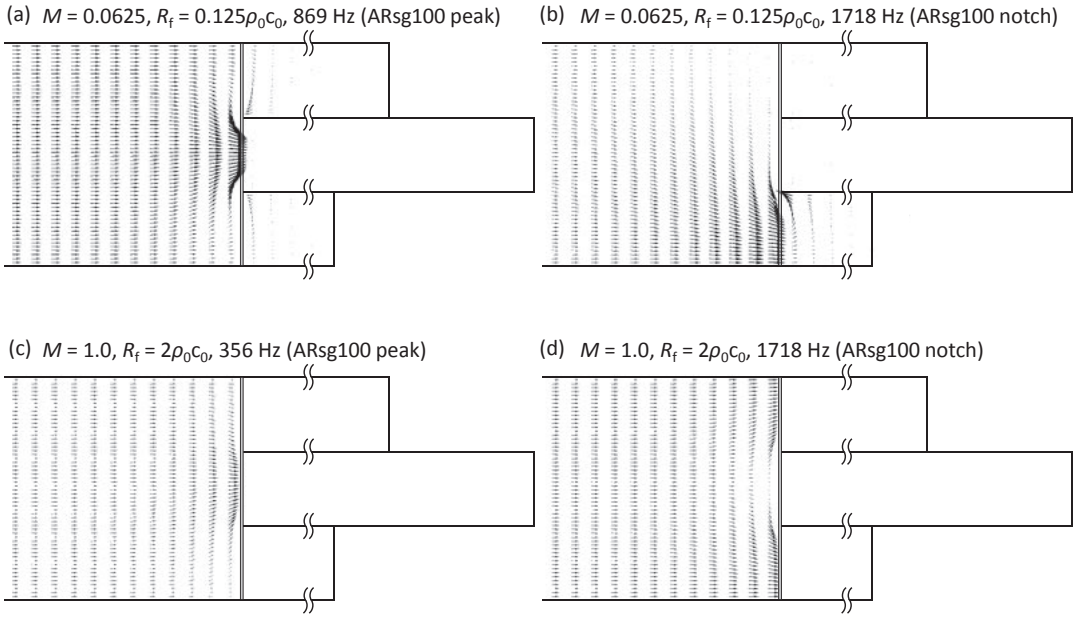

Fig. 6 Acoustic intensity in the tube at frequencies with peak and notch in ARsg100. The results are shown for the cases with $M = 0.0625$ and $R_f = 0.125\rho_0 c_0$ and $M = 1.0$ and $R_f = 2\rho_0 c_0$.

is equal to $\rho_0 c_0$ or $2\rho_0 c_0$, the excess absorption is suppressed due to smaller impedance discontinuity. The particle velocity difference on each ARsg surface is small.

- In the case with low flow resistance, the surface density values of PM do not have an influence on the absorption characteristics of AR. However, the use of heavier membrane is effective to obtain higher absorption at low frequencies when the membrane's flow resistance is equal to $\rho_0 c_0$ or $2\rho_0 c_0$.

Acknowledgment

This work was supported by JSPS KAKENHI Grant No. 15K18167.

References

[1] K. Sakagami, K. Funahashi, Y. Somatomo, T. Okuzono, C. Nishikawa and M. Toyoda, "An experimental study on the absorption characteristics of three-dimensional permeable membrane space absorber," *Noise Control Eng. J.*, **63**, 300–307 (2015).

[2] K. Sakagami, M. Kiyama, M. Morimoto and D. Takahashi, "Detailed analysis of the acoustic properties of a permeable membrane," *Appl. Acoust.*, **54**, 93–111 (1998).

[3] K. U. Ingard, "Sheet absorbers," in *Notes on Sound Absorption Technology* (Noise Control Foundation, New York, 1994), Chap. 1, pp. 1-1–1-16.

[4] M. N. Guddati and B. Yue, "Modified integration rules for reducing dispersion error in finite element methods," *Comput. Methods Appl. Mech. Eng.*, **193**, 275–287 (2004).

[5] T. Sakuma, T. Iwase and M. Yasuoka, "Prediction of sound fields in rooms with membrane materials: Development of a limp membrane element in acoustical FEM analysis and its application," *J. Archit. Plann. Environ. Eng. AIJ.*, **505**, 1–8 (1998).

[6] C. Wang and L. Huang, "On the acoustic properties of parallel arrangement of multiple micro-perforated panel absorbers with different cavity depths," *J. Acoust. Soc. Am.*, **130**, 208–218 (2011).

[7] M. Yairi, K. Sakagami, K. Takebayashi and M. Morimoto, "Excess sound absorption at normal incidence by two micro-perforated panel absorbers with different impedance," *Acoust. Sci. & Tech.*, **32**, 194–200 (2011).